

# EPIPOLAR GEOMETRY OF LINEAR ARRAY SCANNERS MOVING WITH CONSTANT VELOCITY AND CONSTANT ATTITUDE

M. Morgan<sup>a</sup>, K. Kim<sup>b</sup>, S. Jeong<sup>b</sup>, A. Habib<sup>a</sup>

<sup>a</sup> Department of Geomatics Engineering, University of Calgary, Calgary, 2500 University Drive NW, Calgary, AB, T2N 1N4, Canada - (mfmorgan@ucalgary.ca, habib@geomatrics.ucalgary.ca)

<sup>b</sup> Electronics and Telecommunications Research Institute (ETRI), 161 Gajeong-Dong, Yuseong-Gu, Daejeon, 305-350, Korea – (kokim, soo) @etri.re.kr

## PS WG III/1: Sensor Pose Estimation

**KEY WORDS:** Photogrammetry, Analysis, Direct, Modelling, Pushbroom, Sensor

### ABSTRACT:

Image resampling according to epipolar geometry is a prerequisite for a variety of photogrammetric tasks such as image matching, DEM and ortho-photo generation, aerial triangulation, map compilation, and stereoscopic viewing. The resampling process of imagery captured by frame camera has been established and implemented in current Digital Photogrammetric Workstations (DPW). Scanning analogue images or directly using digital cameras can produce digital images, which are the input media for DPW. So far, there is no digital frame camera capable of producing radiometric and geometric resolutions that are comparable to those associated with analogue ones. To overcome such a limitation, linear array scanners have been developed to capture scenes through multiple exposures of few scan lines along the focal plane. This imaging scenario makes the perspective geometry of line cameras more complicated than that of frame images. Moreover, established procedures for resampling frame images according to epipolar geometry are not suitable for scenes captured by linear array scanners. In this paper, the geometry of epipolar lines in scenes captured by linear array scanners moving with constant velocity and constant attitude is analyzed. The choice of this model is motivated by the fact that many scanners can be assumed to follow such trajectory during the short duration of scene capture (especially when considering space borne imaging platforms). The paper starts by establishing the mathematical model describing the shape of epipolar lines in the captured scenes from a platform moving with constant velocity and constant attitude. The paper proceeds by presenting simulated experimental results using scenes captured according to SPOT, IKONOS and three-line camera imaging configurations, where we show the effect of different stereo-coverage methodologies (i.e., tilting the sensor across the track direction – SPOT, tilting the sensor along track – IKONOS, and using three linear array scanners) on the shape of the epipolar lines. For these scenarios, a measure is introduced to quantify the deviation of the resulting epipolar lines from straightness. Small deviations from straightness will allow for better capability of resampling the captured scenes according to epipolar geometry and thus lead to more straightforward subsequent processing (e.g., DEM generation, stereo-viewing, etc.).

## 1. INTRODUCTION

Scenes captured from linear scanners (also called pushbroom scanners or line cameras) have been introduced for their great potential of generating ortho-photos and updating map databases (Wang, 1999). The linear scanners with up-to one-meter resolution from commercial satellites could bring more benefits and even challenges to traditional topographic mapping with aerial images (Fritz, 1995).

Careful sensor modelling has to be adapted in order to achieve the highest potential accuracy. Rigorous modelling describes the scene formation as it actually happens, and therefore it is the most accurate model. Thus, it has been adopted in a variety of applications (Lee and Habib, 2002; Habib et al., 2001; Lee et al., 2000; Wang, 1999; Habib and Beshah, 1998; McGlone and Mikhail, 1981; Ethridge, 1977).

On the other hand, other approximate models exist such as rational function model, RFM, direct linear transformation, DLT, self-calibrating DLT and parallel projection (Tao and Hu, 2001; Ono et al., 1999; Wang, 1999; Abdel-Aziz and Karara, 1971). Selection of any approximate model, as an alternative of rigorous modelling, has to be done based on the analysis of the achieved accuracy. In this paper, rigorous modelling of linear array scanners is adopted.

Epipolar resampling of frame images is a straightforward process (Cho et al., 1992). However, resampling linear array scanner scenes according to epipolar geometry is not a trivial task. The difficulties in resampling the scenes can be, to a certain degree, attributed to the shape of epipolar lines. Therefore, this paper is dedicated to the shape analysis of epipolar lines, and how close they are to straight lines. Kim (2000) investigated the epipolar geometry of linear array scanner scenes. The author concluded that scanners moving according to second order polynomial functions in position and heading angle, and first order polynomial functions in roll and pitch angles do not produce straight lines.

In this paper, Section 2 contains background information regarding frame images as well as linear array scanner scenes. The choice of constant-velocity-constant-attitude as the rigorous sensor model and its utilization in deriving the epipolar line equation are the subjects of Section 3. Section 4 is dedicated to the analysis of the shape of epipolar lines. Experimental results are then presented in Section 5. Finally Section 6 includes the conclusions and recommendations for future work.

## 2. BACKGROUND

### 2.1 Epipolar Geometry of Frame Cameras

#### 2.1.1 Definitions

It is important to list some terms with their definitions before going into any detailed discussion (Cho et al., 1992). These terms will be used throughout the analysis of the epipolar geometry of frame images. Figure 1 shows two frame images, relatively oriented similar to that at the time of exposure.  $O$  and  $O'$  are the perspective centres of the left and right images at the time of exposure, respectively.

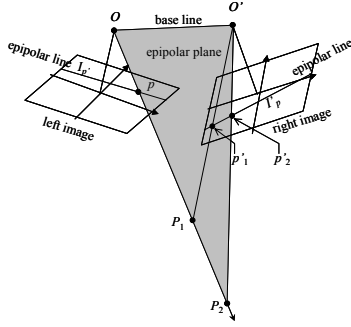


Figure 1. Epipolar geometry in frame images

**Epipolar plane:** The epipolar plane for a given image point  $p$  in one of the images is the plane that passes through the point  $p$  and both perspective centres,  $O$  and  $O'$ .

**Epipolar line:** The epipolar line can be defined in two ways. First, it can be defined as the intersection of the epipolar plane with an image, which produces a straight line. Secondly, the epipolar line can be represented by the locus of all possible conjugate points of  $p$  on the other image (by changing the height of the corresponding object point). The latter definition will be used when dealing with linear array scanners.

It should be noted that no DEM is needed to determine the epipolar line. Selecting several points along the ray ( $Op$ ), i.e., choosing different height values of the object point, will yield the same epipolar line ( $I'_p$ ) in the other image, Figure 1.

Another important property of epipolar lines in frame images is their existence in conjugate pairs. Consider Figure 1, where  $I'_p$  is the epipolar line in the right image for point  $p$  in the left image, and  $p'_1, p'_2$  are two different points in the right image selected on  $I'_p$ . The epipolar lines of points  $p'_1$  and  $p'_2$  will be identical, denoted as  $I_p$ , and will pass through the point  $p$ . This can be easily seen from the figure since all these points and lines should be in the same plane (the epipolar plane).

#### 2.1.2 Epipolar Line Determination in Frame Images

##### Method 1: Collinearity Equations Through the Object Space

The collinearity equations (Kraus, 1993), Equation 1, relate a point in the object space and its corresponding point in the image space.

$$\begin{bmatrix} X_k \\ Y_k \\ Z_k \end{bmatrix} = \begin{bmatrix} X_0 \\ Y_0 \\ Z_0 \end{bmatrix} + \frac{1}{\lambda_k} R \begin{bmatrix} x - x_0 \\ y - y_0 \\ -c \end{bmatrix} \quad (1)$$

Where:

- $x, y$  are the image coordinates of a point in the image;
- $x_0, y_0, c$  are the Interior Orientation Parameters, IOP, of the frame camera;
- $X_0, Y_0, Z_0$  are the position of the exposure station;
- $R$  is the rotation matrix of the image;
- $X_k, Y_k, Z_k$  are the coordinates of the object space point;
- $\lambda_k$  is the scale factor.

Considering Figure 1, two sets of collinearity equations can be written for point  $p$  by setting the scale factor  $\lambda_k$  to two arbitrary values. This results in two arbitrary object space points,  $P_1$  and  $P_2$ , along the ray  $Op$ . The two object points are then re-projected into the right image with known orientation parameters. The resulting points,  $p'_1$  and  $p'_2$ , form the epipolar line.

##### Method 2: Coplanarity Condition Without Visiting the Object Space

The coplanarity condition (Kraus, 1993), Equation 2 can be directly used to determine the epipolar line equation.

$$(OO' \otimes Op) \circ O'p' = 0 \quad (2)$$

Where:

- $OO'$  is the vector connecting the two perspective centres;
- $Op$  is the vector connecting the point of interest  $p$  in the left image with its perspective centre,  $O$ ;
- $O'p'$  is the vector connecting the corresponding point in the right image with its perspective centre; and
- $\otimes, \circ$  symbolize vectors cross and dot products, respectively.

Since only the coordinates of the corresponding point in the right image (i.e.,  $x'$  and  $y'$ ) are unknown, Equation 2 becomes the epipolar line equation. One has to note that in this method, the object space point, or its possible location, has not been dealt with. Next section deals with linear array scanners as alternative to frame cameras.

### 2.2 Linear Array Scanners

#### 2.2.1 Motivations for using Linear Array Scanners

Two-dimensional digital cameras capture the data using two-dimensional CCD array. However, the limited number of pixels in current digital imaging systems hinders their application towards extended large scale mapping functions.

One-dimensional digital cameras (linear array scanners) can be used to obtain large ground coverage and maintain a ground resolution comparable with scanned analogue photographs. However, they capture only one-dimensional image (narrow strip) per snap shot. Ground coverage is achieved by moving the scanner (airborne or space-borne) and capturing many 1D images. The scene of an area of interest is obtained by stitching together the resulting 1D images. It is important to note that every 1D image is associated with one-exposure station, and therefore, each image has its own set of Exterior Orientation Parameters (EOP).

A clear distinction is made between the two terms “scene” and “image” throughout the analysis of linear array scanners.

An **image** is defined as the recorded sensory data associated with one exposure station. In case of a frame image, it contains only one exposure station, and consequently it is one complete image. In case of linear array scanner, there are many 1D

images, each is associated with different exposure stations. The mathematical model that relates a point in the object space and its corresponding point in the image space is the collinearity equations, which uses EOP of the appropriate image (in which the point appears).

In contrast, a **scene** is the recorded sensory data associated with one (as in frame images) or more exposure stations (as in linear array scanners) that maps near-continuous object space in a short single trip of the sensor. Therefore, in frame images, image and scene are identical terms, while in linear array scanners, the scene is an array of consecutive 1D images.

Consequently, it is important to distinguish between the scene and image coordinates. As shown in Figure 2b,  $i$  and  $y$  are the scene coordinates, while in Figure 2a,  $x_i$  and  $y_i$  are the image coordinates for image number  $i$ . Only  $x_i$  and  $y_i$  can be used in the collinearity equations, while  $i$  indicates the image number or the time of exposure.

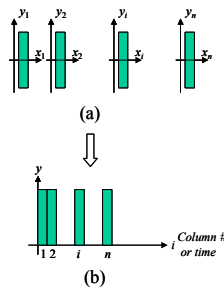


Figure 2. A sequence of 1D images (a) constituting a scene (b)

### 2.2.2 Stereo Coverage

One of the main objectives of photogrammetry is to reconstruct the three-dimensional object space from 2D images/scenes. This is usually achieved by intersecting light rays of corresponding points in different views. Therefore, different views or stereo coverage is essential for deriving 3D information regarding the object space. In linear array scanners, stereo coverage can be achieved using one of the following ways:

- **One scanner and across track stereo coverage using roll angles:** Stereo coverage can be achieved by tilting the camera sideways across the flight direction (different roll angles), Figure 3a. This has been adopted in SPOT. A drawback is the large time gap between images of the stereo pair, and consequently changes may occur between the two scenes (Wang, 1999).
- **One scanner and along track stereo coverage using pitch angles:** In this case the camera is tilted forward and backward along the flight direction (different pitch angles), Figure 3b. This type of stereo coverage is used in IKONOS. This method has the advantage of reducing the time gap between the scenes constituting the stereo pair.
- **Three scanners (three-line cameras):** In this case, three scanners are used to capture backward-looking, nadir, and forward-looking scenes, Figure 3c. Continuous stereo or triple coverage can be achieved along the flight line with reduced time gaps. However, different radiometric qualities exist between the scenes. This method is implemented in MOMS and ADS40 (Heipke et al., 1996; Sandau et al., 2000; Fraser et al., 2001).

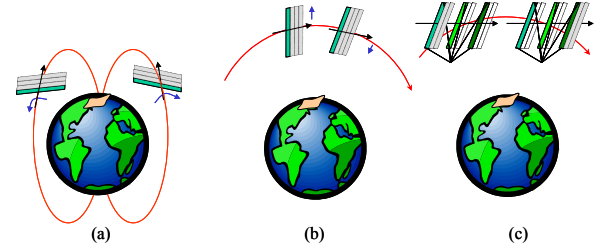


Figure 3. Stereo coverage in linear array scanners achieved by roll angle rotation in two flying paths (a), pitch angle rotation in the same flying path (b), and three-line cameras (c).

### 2.2.3 Rigorous Modelling

Rigorous (exact) modelling of linear array scanners describes the actual geometric formation of the scenes at the time of photography, that requires the knowledge of IOP of the scanner and the EOP of each image in the scene. Usually, EOP do not abruptly change their values between consecutive images in the scene, especially for space-based scenes. Therefore, most rigorous modelling methods adapt polynomial representation of EOP (Lee et al., 2000; Wang, 1999). The parameters, describing the polynomial functions, are either given (directly) from the navigation units such as GPS/INS mounted on the platform, or indirectly estimated using ground control in bundle adjustment (Lee and Habib, 2002; Habib et al., 2001; Habib and Beshah, 1998). Other methods (Lee et al., 2000; McGlone and Mikhail, 1981; Ethridge, 1977) use piecewise polynomial model for representing the flight trajectory and the platform attitude. This option is preferable if the scene time is large, and the variations of EOP do not comply with one set of polynomial functions.

For indirect estimation of the polynomial coefficients using ground control points, instability of the bundle adjustment exists, especially for space-based scenes (Fraser et al., 2001; Wang, 1999). This is attributed to the narrow Angular Field of View (AFOV) of space scenes, which results in very narrow bundles in the adjustment procedures. To avoid the polynomial representation of EOP, Lee and Habib (2002) explicitly dealt with all EOP associates with the scene. Linear feature constraints were used to aid independent recovery of the EOP of the images as well as to increase the geometric strength of the bundle adjustment.

## 2.3 Epipolar Geometry of Linear Array Scanner Scenes

Kim (2000) modelled the changes of EOP as second order polynomial functions in scanner position and heading, and first order functions in pitch and roll angles. This model is called “Orun and Natarajan” model as cited from (Orun and Natarajan, 1994). The author proved that the epipolar line is no longer a straight line, rather has hyperbola-like shape. In addition, the author proved that epipolar lines do not exist in conjugate pairs. The next section investigates the epipolar geometry of linear array scanners using constant-velocity-constant-attitude EOP model, which is a subclass of “Orun and Natarajan” model. But first, epipolar line determination in linear array scanners has to be explained.

As discussed earlier, scanner at successive exposure stations has different perspective centres and different attitude, therefore, EOP will vary from one scan line to the other. Hence, the epipolar lines should be clearly defined in such scenes before studying their geometry. Figure 4 shows a schematic drawing of

two linear array scanner scenes. For a 1D image in the left scene with  $O$  as its perspective centre, point  $p$  can correspond to many epipolar planes (unlike the case of frame images - compare Figures 1 and 4). In this case, there are as many epipolar planes as the perspective centres in the right scene. Therefore, the epipolar line cannot be defined as the intersection of planes. Instead, the second definition used in frame images is adopted, where the epipolar line is defined as the locus of all possible conjugate points of  $p$  on the other scene based on the orientation parameters.

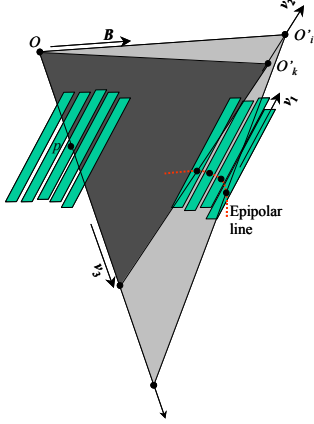


Figure 4. Epipolar line in linear array scanner scenes

In order to determine the epipolar line, EOP of the scan lines together with the IOP of the scanner must be available. The epipolar line can be determined in a similar way as discussed in Section 2.1.2 by repeating the procedure for each scan line since each scan line has different EOP. The change in EOP from one scan line to the next is one of the factors that determine the shape of the epipolar line.

### 3. UTILIZING CONSTANT VELOCITY AND CONSTANT ATTITUDE MODEL

The motivation of investigating the constant-velocity-constant-attitude model is that many space scenes are acquired in very short time (e.g., about one second for IKONOS scene). In addition, similar assumptions were made for EOP when deriving the SDLT model for linear array scanners (Wang, 1999). The scanner, therefore, can be assumed to travel with constant velocity and constant attitude during the scene capture, Equations 3.

$$\begin{bmatrix} X_{0j} = X_0 + \Delta X \cdot j \\ Y_{0j} = Y_0 + \Delta Y \cdot j \\ Z_{0j} = Z_0 + \Delta Z \cdot j \\ \kappa_j = \kappa \\ \omega_j = \omega \\ \varphi_j = \varphi \end{bmatrix}, \begin{bmatrix} X'_{0i} = X'_0 + \Delta X' \cdot i \\ Y'_{0i} = Y'_0 + \Delta Y' \cdot i \\ Z'_{0i} = Z'_0 + \Delta Z' \cdot i \\ \kappa'_i = \kappa' \\ \omega'_i = \omega' \\ \varphi'_i = \varphi' \end{bmatrix} \quad (3)$$

where:

$j$  is the scan line number on the left scene;  
 $i$  is the scan line number on the right scene;  
 $(X_0, Y_0, Z_0)$  is the position of the first exposure station in the left scene;

$(\Delta X, \Delta Y, \Delta Z)$  is the constant velocity vector of the scanner while capturing the left scene;  
 $(X'_0, Y'_0, Z'_0)$  is the position of the first exposure station in the right scene;  
 $(\Delta X', \Delta Y', \Delta Z')$  is the constant velocity vector of the scanner while capturing the right scene;  
 $(\omega, \varphi, \kappa)$  are the rotation angles of the left scanner; and  
 $(\omega', \varphi', \kappa')$  are the rotation angles of the right scanner.

For a point  $(j, y_j)$  on the left scene, the collinearity equations can be written as:

$$\begin{aligned} X &= A_1 \cdot Z + A_2 \\ Y &= A_3 \cdot Z + A_4 \end{aligned} \quad (4)$$

where  $A_1$  to  $A_4$  are functions of the IOP and EOP of the left scene. Equation 4 represents two planes parallel to  $Y$  and  $X$  axes, respectively. Their intersection is a straight-line (a light ray in space). On the other hand, for the right scene, the collinearity equations are:

$$\begin{bmatrix} x' - x_0 \\ y'_i - y_0 \\ -c \end{bmatrix} = \lambda'_i R^{iT}_{i(\omega'_i, \varphi'_i, \kappa'_i)} \begin{bmatrix} X - X'_{0i} \\ Y - Y'_{0i} \\ Z - Z'_{0i} \end{bmatrix} \quad (5)$$

Using EOP from Equations 3, and substituting for  $X$  and  $Y$  from Equation 4, Equations 5 can be written as:

$$y'_i \cdot E_1 + y_i \cdot E_2 = i \cdot E_3 + E_4 \quad (6)$$

where  $E_1$  to  $E_4$  are functions of the IOP and EOP of the scanner. Detailed derivation of the above equation can be found in (Morgan, 2004).

### 4. ANALYSIS OF EPIPOLAR LINES

Equation 6 represents the locus of potential conjugate points in the right scene (i.e., the equation of the epipolar line in the right scene). It is important to note that  $y'_i$  is unknown (at image number  $i$ ). The epipolar curve is a straight line if  $E_2=0$ , hence  $y'_i$  is a linear function of  $i$ . Therefore, the term  $E_2$  has to be analyzed. Setting  $E_2$  to 0, the condition for having the epipolar curve as a straight line can be expressed as triple product of three vectors  $\mathbf{v}_1$ ,  $\mathbf{v}_2$  and  $\mathbf{v}_3$ , Figure 4, as:

$$(\mathbf{v}_1 \otimes \mathbf{v}_2) \circ \mathbf{v}_3 = 0 \quad (7)$$

Equation 7 indicates that these three vectors, shown in Figure 4, must be coplanar in order to have the epipolar curve as a straight line. In reality, it is hard to find the above condition valid and equals to absolute zero. In order to quantify the straightness of the epipolar curve, the value of  $E_2$  has to be compared to the value of  $E_1$ . The smaller the ratio of  $(E_2/E_1)$ , the epipolar curve will become closer to being straight.

$$\frac{E_2}{E_1} = \frac{(\mathbf{v}_1 \otimes \mathbf{v}_2) \circ \mathbf{v}_3}{(\mathbf{v}_1 \otimes \mathbf{B}) \circ \mathbf{v}_3} \quad (8)$$

where  $\mathbf{B}$  is the airbase vector, connecting the perspective point of the point under consideration in the left scene and the perspective centre of the first image in the right scene. Recall that epipolar lines in frame images are straight lines in both the

raw and normalized images. Therefore, no distortions are introduced in such a process. On the other hand, in linear array scenes, epipolar lines may not be straight, but it is desirable to have them as straight lines in the normalized scenes. Therefore, the evaluation of their non-straightness in the raw scenes will give an idea about the errors introduced in the normalized scenes.

## 5. EXPERIMENTS

In order to study the epipolar geometry, two scenes are needed. Nine experiments are performed. Experiments 1, 2 and 3 are simulated to obtain stereo coverage for a three-line camera, at different altitudes. On the other hand, Experiments 4, 5 and 6 are simulated to obtain stereo coverage by changing the pitch angles along track similar to that of IKONOS, at different altitudes. Finally, Experiments 7, 8 and 9 are simulated to obtain stereo coverage by changing roll angles across track similar to that of SPOT at different altitudes. The summary of the experiments is listed in Table 1. Figure 6 shows the footprints of the scan lines of the scenes.

		Altitude		
		1000 m	680 km	822 km
Stereo coverage method	Three-line scanner	Exp. 1	Exp. 2	Exp. 3
	Changing pitch angle	Exp. 4	Exp. 5	Exp. 6
	Changing roll angle	Exp. 7	Exp. 8	Exp. 9

Table 1. Summary of Experiments 1 to 9

In each of these experiments, five points are selected in the left scene. Figure 7 shows the corresponding epipolar lines of the experiments. The epipolar lines are drawn within the extent of the right scenes. Dotted straight lines are added between the beginning and ending points to visually examine the straightness of these epipolar lines. It has been found that  $E_2$  does not equal zero. Therefore, for general linear array scanner (even with the constant-velocity-constant-attitude trajectory model), the epipolar lines are not straight. In order to quantify the straightness of epipolar lines, Table 2 lists the values of  $E_2/E_1$  for the experiments.

Examining the standard deviation of  $E_2/E_1$  of the selected points in each experiment, it is noticeable that  $E_2/E_1$  values do not change from point to point in the scene in Experiments 1 to 6. This means that these epipolar lines, even if they are not straight lines, are changing in a similar fashion. On the other hand, the standard deviations of  $E_2/E_1$  values in Experiments 7 to 9 are relatively large, which consequently means that there is a high variation of the shapes of the epipolar lines. This is confirmed by extreme example, Experiment 7 in Figure 7. Therefore, it can be concluded that stereo coverage similar to that of three-line camera or IKONOS are superior, in terms of shape variation of epipolar lines, to that of SPOT.

Examining the average values of  $E_2/E_1$ , it is noticeable that  $E_2/E_1$  decreases as the altitude increases, for the same stereo coverage type. Moreover, stereo coverage similar to IKONOS or three-line cameras gives smaller average values than that of SPOT at the same altitude (Compare the average values of Experiments 1, 4 and 7; those of Experiment 2, 5 and 8, and finally those of Experiments 3, 6 and 9).

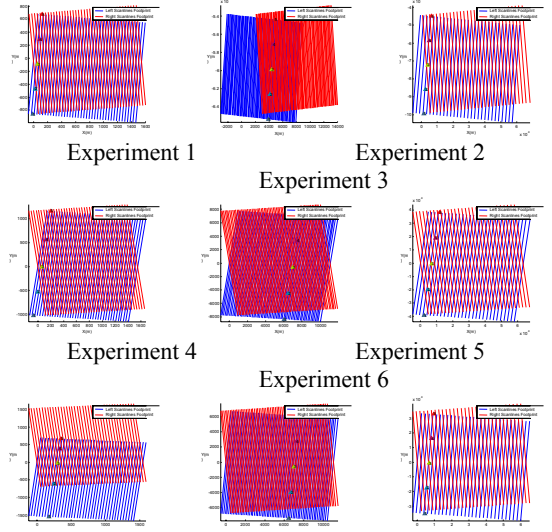


Figure 6. Scan lines footprints of Experiments 1 to 9

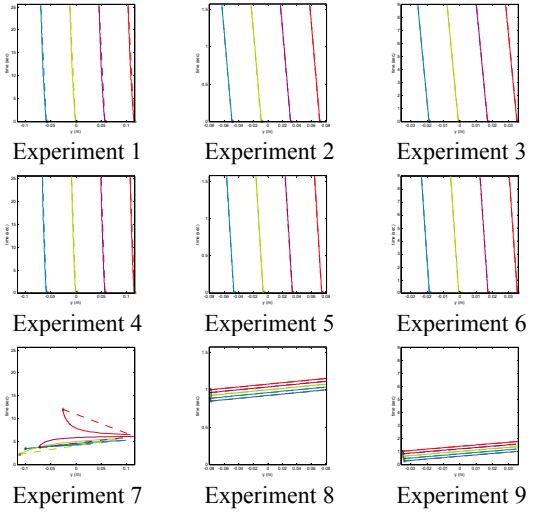


Figure 7. Epipolar lines of Experiments 1 to 9

	Point#	1	2	3	4	5	Mean $\pm$ Std
Experiment	1	0.031	0.031	0.031	0.031	0.031	0.031 $\pm$ 0.000
	2	0.005	0.005	0.005	0.005	0.005	0.005 $\pm$ 0.000
	3	0.004	0.004	0.004	0.004	0.004	0.004 $\pm$ 0.000
	4	0.031	0.031	0.031	0.031	0.031	0.031 $\pm$ 0.000
	5	0.005	0.005	0.005	0.005	0.005	0.005 $\pm$ 0.000
	6	0.004	0.004	0.004	0.004	0.004	0.004 $\pm$ 0.000
	7	-0.012	-0.114	-0.144	-0.158	-0.167	-0.119 $\pm$ 0.063
	8	-0.076	-0.077	-0.077	-0.077	-0.078	-0.077 $\pm$ 0.001
	9	-0.062	-0.063	-0.065	-0.066	-0.067	-0.065 $\pm$ 0.002

Table 2.  $E_2/E_1$  values for various points in Experiments 1 to 9

## 6. CONCLUSIONS AND RECOMMENDATIONS

It has been concluded that for constant-velocity-constant-attitude EOP model, the epipolar line is found to be a non-straight line in general and a quantitative analysis of its non-straightness was introduced. Analysis of alternative stereo-coverage possibilities revealed that along track stereo observation using pitch angles as well as three-line scanners are

superior to across track stereo coverage using roll angles as they introduce straighter epipolar lines. Moreover, as the flying height increases, epipolar lines become straighter. Such conclusions motivate the investigation of epipolar resampling of space scenes such as IKONOS.

As the derived quantitative measure examines the straightness of epipolar lines without restriction to the scene extent, different measure has to be introduced to examine their quality within the scenes.

On the other hand, as the general EOP model does not result in straight epipolar lines, different models have to be sought for the purpose of epipolar resampling of linear array scanner scenes.

## REFERENCES

- Abdel-Aziz, Y., and H. Karara, 1971. Direct Linear Transformation from Comparator Coordinates into Object Space Coordinates in Close-Range Photogrammetry, *Proceedings of ASP/UI Symposium on CloseRange Photogrammetry*, University of Illinois at Urbana Champaign, Urbana, Illinois, pp. 1-18.
- Cho, W., T. Schenk, and M. Madani, 1992. Resampling Digital Imagery to Epipolar Geometry, *IAPRS International Archives of Photogrammetry and Remote Sensing*, 29(B3): 404-408.
- Ethridge, M., 1977. *Geometric Analysis of Single and Multiply Scanned Aircraft Digital Data Array*, PhD Thesis, Purdue University, West Lafayette, Indiana, 301p.
- Fraser, C., H. Hanley, and T. Yamakawa, 2001. Sub-Metre Geopositioning with IKONOS GEO Imagery, *ISPRS Joint Workshop on High Resolution Mapping from Space*, Hanover, Germany, 2001.
- Fritz, L., 1995. Recent Developments for Optical Earth Observation in the United States, *Photogrammetric Week*, pp75-84, Stuttgart, 1995.
- Habib, A. and B. Beshah, 1998. Multi Sensor Aerial Triangulation, *ISPRS Commission III Symposium*, Columbus, Ohio, 6 – 10 July, 1998.
- Habib, A., Y. Lee, and M. Morgan, 2001. Bundle Adjustment with Self-Calibration of Line Cameras using Straight Lines, *Joint Workshop of ISPRS WG I/2, I/5 and IV/7: High Resolution Mapping from Space 2001*, University of Hanover, 19-21 September, 2001.
- Heipke, C., W. Kornus, and A. Pfannenstien, 1996. The Evaluation of MEOSS Airborne Three-Line Scanner Imagery: Processing Chain and Results, *Journal of Photogrammetric Engineering & Remote Sensing*, 62(3): 293-299.
- Kim, T., 2000. A Study on the Epipolarity of Linear Pushbroom Images, *Journal of Photogrammetric Engineering & Remote Sensing*, 66(8): 961-966.
- Kraus, K. 1993. *Photogrammetry*, Dümmler Verlag, Bonn., Volume 1, 397p.
- Lee, Y., and A. Habib, 2002. Pose Estimation of Line Cameras Using Linear Features, *ISPRS Symposium of PCV'02 Photogrammetric Computer Vision*, Graz, Austria.
- Lee, C., H. Theiss, J. Bethel, and E. Mikhail, 2000. Rigorous Mathematical Modeling of Airborne Pushbroom Imaging Systems, *Journal of Photogrammetric Engineering & Remote Sensing*, 66(4): 385-392.
- McGlone, C., and E. Mikhail, 1981. Photogrammetric Analysis of Aircraft Multispectral Scanner Data, *School of Civil Engineering, Purdue University*, West Lafayette, Indiana, 178p.
- Morgan, M., 2004. *Epipolar Resampling of Linear Array Scanner Scenes*, PhD Dissertation, Department of Geomatics Engineering, University of Calgary, Canada.
- Ono, T., Y. Honmachi, and S. Ku, 1999. Epipolar Resampling of High Resolution Satellite Imagery, *Joint Workshop of ISPRS WG I/1, I/3 and IV/4 Sensors and Mapping from Space*.
- Orun, A., and K. Natarajan, 1994. A Modified Bundle Adjustment Software for SPOT Imagery and Photography: Tradeoff, *Journal of Photogrammetric Engineering & Remote Sensing*, 60(12): 1431-1437.
- Sandau, R., B. Braunecker, H. Driescher, A. Eckardt, S. Hilbert, J. Hutton, W. Kirchhofer, E. Lithopoulos, R. Reulke, and S. Wicki, 2000. Design Principles of the LH Systems ADS40 Airborne Digital Sensor, *International Archives of Photogrammetry and Remote Sensing*, Amsterdam, 33(B1): 258-265.
- Tao, V. and Y. Hu, 2001. A Comprehensive Study for Rational Function Model for Photogrammetric Processing, *Journal of Photogrammetric Engineering & Remote Sensing*, 67(12):1347-1357.
- Wang, Y., 1999. Automated Triangulation of Linear Scanner Imagery, *Joint Workshop of ISPRS WG I/1, I/3 and IV/4 on Sensors and Mapping from Space*, Hanover, 1999.